



Seatific

<https://seatific.yildiz.edu.tr>

DOI: <https://doi.org/10.14744/seatific.2022.0004>

Seatific

Research Article

Developing an experimental method to investigate hydrodynamic drag

Serkan Türkmen^{*1}, Mehmet Atlar², Irma Yeginbayeva³

¹Newcastle University Faculty of Engineering, Marine, Offshore & Subsea Technology Group, Newcastle upon Tyne, UK

²Department of Naval Architecture Ocean and Marine Engineering, University of Strathclyde, Glasgow, UK

³Fouling Protection, Jotun, Sandefjord, Norway

ARTICLE INFO

Article history

Received: February 09, 2022

Revised: June 17, 2022

Accepted: June 29, 2022

Key words:

Biofouling; Drag; Flow cell;
Roughness

ABSTRACT

Newcastle University [UNEW] has enhanced the test section of their existing water channel facility. The new measurement section is utilized to measure pressure drop (and hence frictional drag) across a standard flat test panel (length=0.6 m; width=0.22 m). The panel can be tested as cleanly coated as well as exposed to light biofilm growth. Based on measured pressure gradients, the skin friction coefficients of these surfaces are calculated and compared with other well-established methods (i.e., measuring the boundary layer of similar surfaces using a [LDV] system in UNEW's Emerson Cavitation Tunnel [ECT]), to evaluate the pressure drop methodology. This paper presents a design and calibration of a flow cell to investigate skin-friction of three different surfaces in a fully developed turbulent flow.

Cite this article as: Türkmen S, Atlar M, Yeginbayeva I, Benson S. Developing an experimental method to investigate hydrodynamic drag. *Seatific* 2022;2:1:44–51.

1. INTRODUCTION

One of the main parameters apart from wave-making that affects the total resistance when dealing with a submerged section of a sailing vessel's hull is frictional resistance. Frictional resistance is caused by normal and tangential components of the viscous flow. The normal component of the viscous resistance is affected by hull shape, which the literature refers to as form factor. The tangential component of viscous resistance (shear stress) runs parallel to the ship's hull and causes a net force opposite the direction of motion. This phenomenon is also called skin friction (Harvald,1983).

Ship operators pay an economic penalty as a result of marine biological fouling on the hull. For instance, skin friction can increase by 30-40% based solely on light or hard fouling,

which leads to greater fuel consumption and reduced operating speed (Woods Hole Oceanographic Institution, 1952; Townsin, 2003; Banerjee et al., 2011; Schultz et al., 2011). In fact, increased fuel consumption causes further trouble as the vessel is not able to satisfy the mandatory regulations for ship carbon emissions (e.g., Energy Efficiency Design Index, Ship Energy Efficiency Management Plan).

Marine coatings are essential to prevent biofouling from developing on ships. Self-polishing co-polymer (SPC) and foul-release (also known as non-stick, low surface energy) silicone elastomers have been the most common antifouling coatings since tributyltin (TBT) was completely banned from application in 2003. The effectiveness of a coated hull surface may differ due to hydraulic roughness and aging

*Corresponding author.

*E-mail address: serkan.turkmen@ncl.ac.uk



Published by Yıldız Technical University Press, İstanbul, Türkiye

This is an open access article under the CC BY-NC license (<http://creativecommons.org/licenses/by-nc/4.0/>).

in addition to fouling. Developing test methodologies for evaluating the hydrodynamic performance of fouling control coatings is particularly complex. Several established methods exist for assessing the hydrodynamic performance of a rough and bio-filmed surface (Candries, 2001; Politis et al., 2013). This development needs to be designed in such a way as to replicate the physical and environmental conditions the coating will experience when applied on the surface of a ship hull. The most common techniques include rectangular flow channels, circulating water tunnels, towing tanks, axi-symmetrical slender bodies, and the rotating disk and drum Taylor-Couette flow facility. Among these rectangular flow channels, generally known as flumes or flow cells, the turbulent water flow channel is a fast and economical method to test such coatings.

Newcastle University enhanced the pressure-drop flume by replacing its measuring section with a sophisticated pressure-drop facility to assess the skin friction characteristics of a standard test panel (0.6m length×0.22m width×0.015m height), which allows easy transportation. The dimensions of the panels were chosen for compatibility with Newcastle University's various facilities (i.e., the Cavitation Tunnel, flowcell, coating ageing flume, slime farm, and strut arrangement of the research vessel, RV the Princess Royal; Politis et al., 2013).

The test panels containing the biofilm samples can be transferred to the UNEW testing facilities in the shortest time in wet containers for hydrodynamic testing once the required amount of biofilm has been collected. Therefore, clean and biofouled flat panels can be tested to measure their skin friction in fully turbulent flows using modern experimental facilities, which is more robust and attractive.

The main purpose of this device is to investigate the skin friction characteristics of flat test panels; these can be non-coated or coated, as well as clean or subjected to biofilm under seawater conditions. This paper presents the design and calibration process of a flow cell. Further tests have been conducted to investigate skin friction of three surface coatings with different roughness profiles. The results have been given to correlate the roughness and hydrodynamic drag performance as evaluated by the flow cell.

2. FLOW CELL AND EXPERIMENTAL APPARATUS

2.1. UNEW's flow cell

Figure 1 shows the layout of the new pressure-drop measurement section of this facility and test panel arrangements. As shown in Figure 1, the measurement section is made of stainless steel with a length of 2.7 m installed between a contraction section with a contraction (cross-sectional area) ratio of 34.7:1 and the settling tank. Two identical test panels can be placed at the top and bottom of the pressure-drop section. The rectangular measurement

section has a channel height of 10 mm and width of 180 mm, which shows a width-to-height ratio of 18:1. This high aspect ratio ensures the channel flow is two-dimensional (Dean 1978, Zanoun et al., 2009). The length-to-height ratio is 270 mm, which is much higher than the recommended channel length for fully developed turbulent flow (Monty 2005). The panel surfaces are flush with the inner walls of the testing section to ensure the channel height remains constant.

Figure 2 shows a picture of this new stainless-steel test section installed on the existing flow cell circuit with the new contraction section. A very rigid frame (in blue) supports the heavy stainless-steel section which provides a much more rigid, level, and steady water channel as opposed to the old, uneven, and brittle acrylic measuring section that was at the end of its working life.

The new pressure-drop section has a 150 mm long glass window at one side that can be used to measure the flow velocity profiles between the test panels using LDV or other optical devices (e.g., particle image velocimetry). Four pressure taps are found on the bottom wall and nine pressure taps on one of the side walls of the test section; these enable a wide range of pressure-drop data to be collected using differential pressure transducers. An inspection hatch that replicates the hatch for housing the test panels is also installed upstream of the latter hatch for cleaning and maintaining purposes.

2.2. Measuring equipment

Pressure-drop measurements are taken using differential pressure transmitters (transducers) over various pressure ranges. Water temperature is monitored during the tests to avoid extreme rises in temperature. The inflow speed measured in the test section is presented as a function of the pump speed. In fact, the calibration curves that will be mentioned in Section 3.1 are represented in this manner. A data acquisition system [DAQ] is used to log both pump speed and pressure-drop values.

The flow cell has a 15kW pump able to provide a flow rate up to 300 l/s. In practice, the user relates the channel inflow speed to the pump speed as stated in the calibration curve.

Differential-type pressure sensors are used to measure the pressure differences (pressure drop) between the two interchangeable pressure taps. The range of the pressure drop is calculated using computational fluid dynamics. Two XMD differential pressure transmitters are installed with ranges from 0-75 mbar and 0-500 mbar with an accuracy of 0.1%. The pressure drop data is recorded at a sampling rate of 10 Hz. An overview of the data logging system and measurement equipment for the pump speed and pressure drop is given in Figure 3.

2.3. Calibration

Calibration has two main objectives. The first is to relate the flow details (i.e., flow velocity and turbulence components

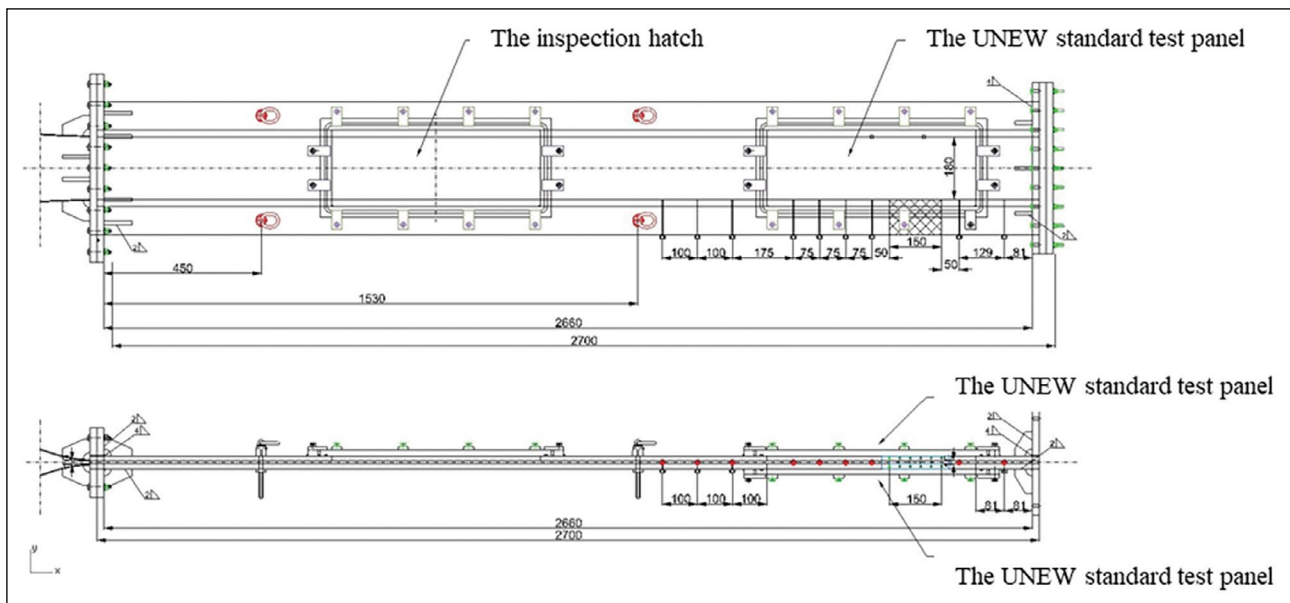


Figure 1. Pressure-drop section with contraction (inlet) and discharge (outlet).



Figure 2. A view of the new test section of UNEW's flow cell.

as well as pressure drop) over the smooth reference surface at the measuring section over the entire range of the main pump speeds due to pump speed being the most practical driver for the flow cell user.

A flume is expected to be able to generate a fully developed turbulent flow over the panels. This is possible when the measurement section is long enough. In addition to the dimensions of the standard panel being significantly larger than the former test panels (75 mm×25 mm microscopic slides), the flow field is now measured at various cross

sections along the measurement area. Therefore, the second objective of the calibration is to prove a fully developed turbulent flow has been generated in the measurement area.

The hydrodynamic characteristics of the flow in the measurement area are captured using the Dantec Dynamic's 2D LDV system. Although other flow measurement devices are found (e.g., pitot tubes, hot wire anemometry, ultrasonic devices), the LDV system has the greatest advantage of being a non-intrusive device as well as one that takes time-dependent point measurements at any specific point.

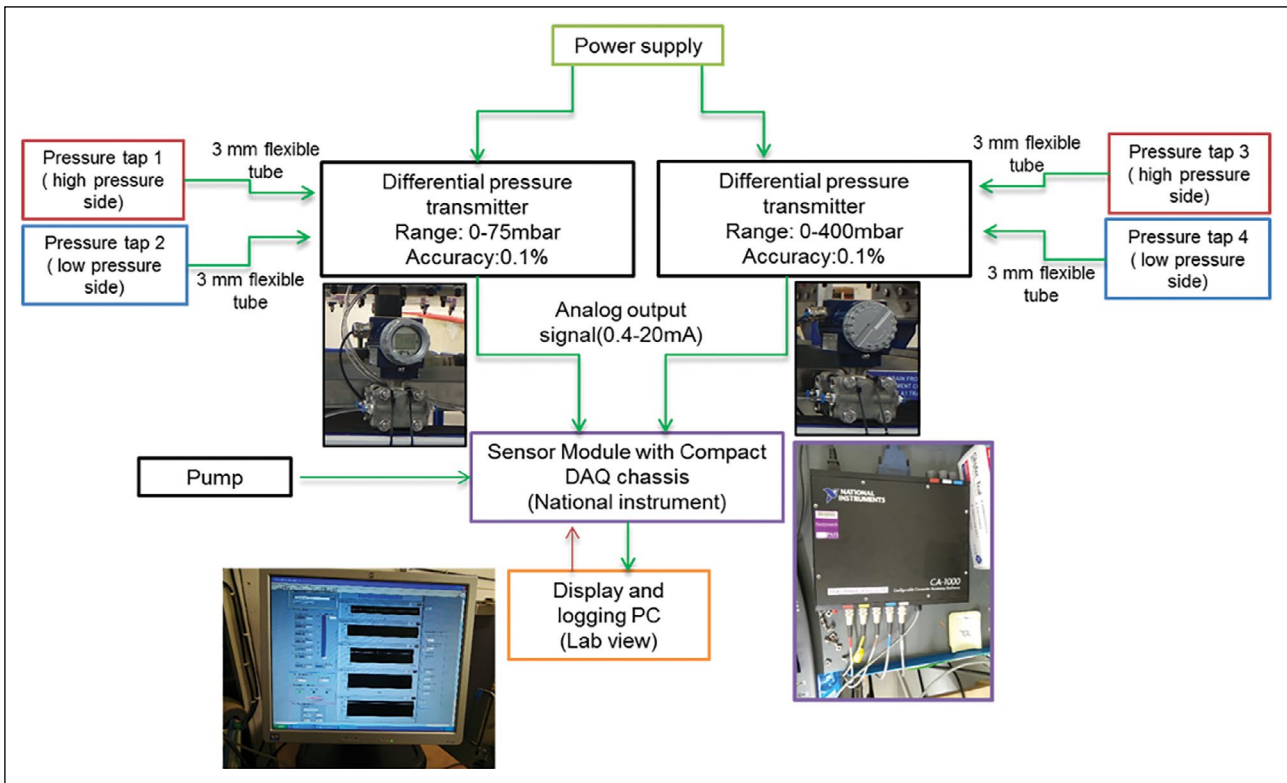


Figure 3. Experimental apparatus layout for main pump speed drive and pressure data logging.

The flow cell was filled with fresh water for the calibration, and the water was seeded for the LDV with silver-coated glass particles with a size of 2 μm .

LDV measurements were taken at three longitudinally selected frames (150 mm intervals) and nine transverse positions (22.5 mm intervals). The location of the measurement points is demonstrated in Figure 4. Figure 5 shows the LDV probe (500 mm focal length) and computer-controlled traverse that drives the LDV probe at any desired point(s) with great accuracy and efficiency. During the calibrations, the traverse was located next to the measurement area for easy access. The flow velocity components (i.e., streamwise [U] and transverse [V]), as well as their respective turbulence intensities, were measured at these points.

Monty (2005) stated that a study comparing turbulence statistics at a number of streamwise stations was necessary to determine the point of full development. Figure 6 presents the flow speed in the streamwise [U] and transverse [V] directions, respectively, for a pump speed of 600 rpm. Figure 7 shows the U velocity vector distribution in the vertical and transverse directions at the three different longitudinal positions (Pos1, Pos2, and Pos3) overlapping with the mean U velocities at these positions. Calibration tests showed the new test section to be able to effectively develop fully turbulent flow at the pressure-drop measurement section.

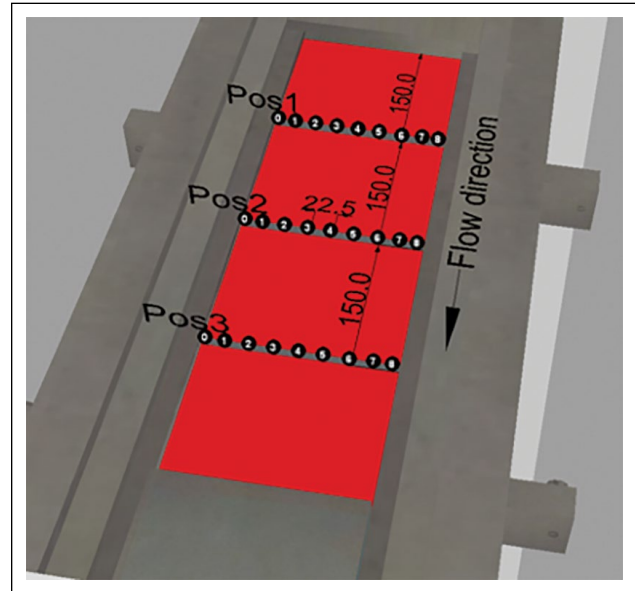


Figure 4. Locations of flow measurement points along the pressure drop section.

3. THE PRESSURE DROP METHODOLOGY

In order to obtain the static pressure gradient $\frac{dp}{dx}$ (ratio of the pressure drop per unit length), the pressure drop (i.e., $p_1 - p_2$) is divided by the observation length l (distance between the taps in the side of the channel).

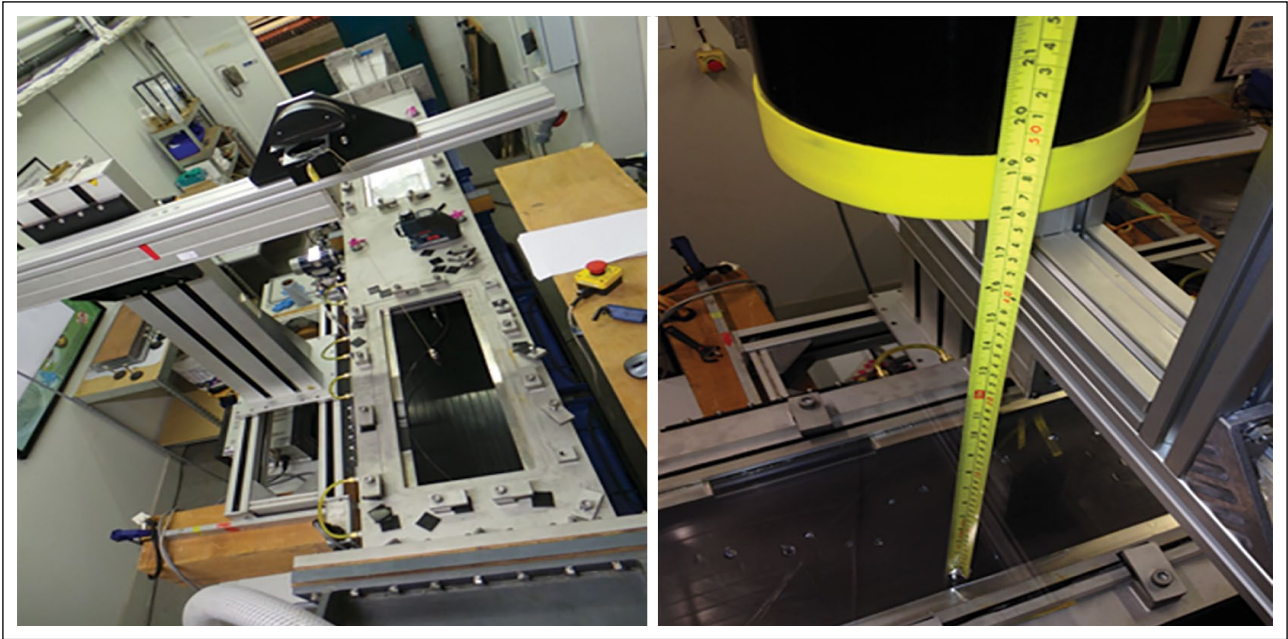


Figure 5. LDV's traverse arrangement during calibration.

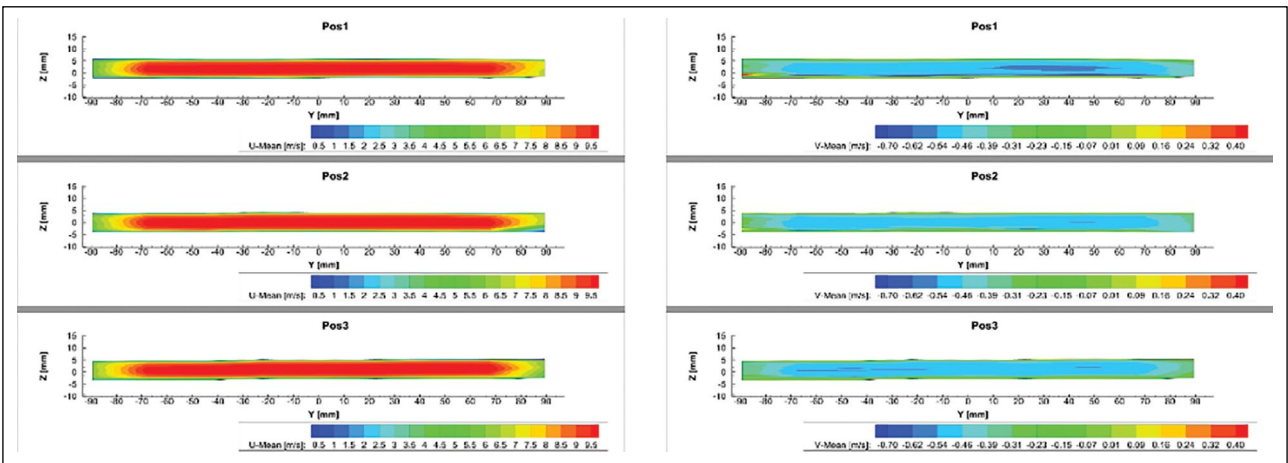


Figure 6. The flow speed along the U (right) and V (left) axes at a pump speed of 1,600 rpm.

The relationship between the wall shear stress (τ_w) and the static pressure gradient can be obtained using Equation 1 (Nikuradse, 1933).

$$\tau_w = -\frac{H dp}{2 dx} \quad (1)$$

where H is the channel height, dp is the pressure difference between the two pressure taps, and dx is the distance between the two pressure taps used to measure the pressure differences. The friction velocity u_τ is introduced as a function of the wall shear stress and density.

$$u_\tau = \left(\frac{\tau_w}{\rho}\right)^{0.5} \quad (2)$$

where water density ρ is taken as 998 kg/m³ (water temperature=20°C). The friction coefficient C_f for a

rectangular duct is defined as a function of the wall shear stress, bulk (mean) velocity \bar{U} , and fluid density:

$$C_f = \left(\frac{\tau_w}{0.5\rho\bar{U}^2}\right) \quad (3)$$

The skin friction coefficient C_f can be rewritten from Equation 2 and Equation 3 as:

$$C_f = 2 \left(\frac{u_\tau}{\bar{U}}\right)^2 \quad (4)$$

Reynold's number can be also described based on the full height (H) of the measurement section and bulk mean velocity \bar{U} (or mean velocity):

$$Re_m = \frac{(H\bar{U})}{\nu} \quad (5)$$

where ν is the kinematic viscosity of water (1.004×10⁻⁶ m²/s).

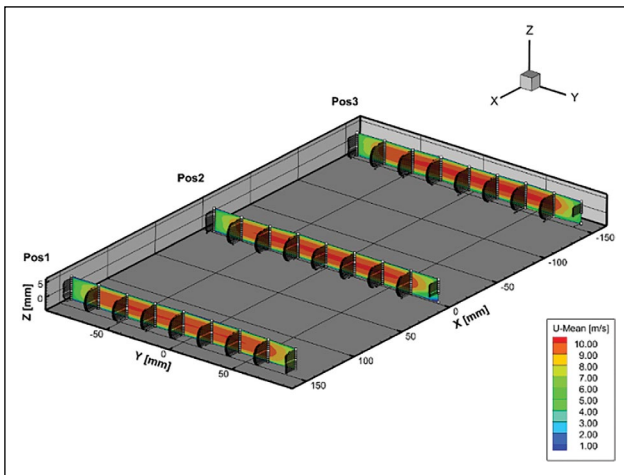


Figure 7. Development of the velocity boundary layer between target plates at a pump speed of 1,600 rpm.

3.1. Description of test surfaces

In order to evaluate the pressuredrop methodology, static pressure-drop data were measured over the following three different surfaces:

1. Hydrodynamically smooth, clean acrylic panel, referred to as the reference surface and indicated as Surface A in the presentations,
2. Clean, newly applied foul-release [FR] coated panel to represent a low-to-medium range rough surface, indicated as Surface B in the presentations, and
3. Clean, newly applied self-polishing copolymer [SPC] coated panel with introduced extra roughness to

represent a rough surface, indicated as Surface C in the presentations.

The three surfaces, each in two replicates of the UNEW test panels, were placed onto the flow cell pressure-drop section for calibration as shown in the top-left panel (replicate 1 of Surface A), and bottom-right panel (replicate 2 of Surface A) in Figure 8.

3.2. Roughness measurements

The roughness measurements of the three surfaces were carried out using Uniscan’s OSP100 device. This instrument is a non-contact, laser-based, high accuracy surface profiling system used to measure and analyze roughness. The arithmetic mean of roughness (R_a) is the general way to describe general surface roughness. From the measured surface profiles the mean R_a values are calculated by comparing all the peaks and valleys to the mean line and then averaged over the entire cut-off length of 5 mm. Table 1 shows the results of the mean R_a values as well as other roughness parameters of the three measured surfaces. Surface A, the clean acrylic surface, provides the smallest R_a of $0.72 \mu\text{m}$ as being the hydraulically smooth reference surface. The R_a value for Surface B (low-to-medium rough surface) is $1.94 \mu\text{m}$, representing a newly coated foul-release surface. The third surface, Surface C, is the roughest, with an average R_a value of around $29 \mu\text{m}$ and representing a coated surface under “in-service” conditions.

4. MEASUREMENTS, ANALYSES, AND RESULTS

The pressure-drop measurements were carried out for a range of pump speeds. Equation 5 was used to calculate



Figure 8. Two parallel smooth test panels (Surface A and its replicate) in place, top panel (L); bottom panel (R).

Table 1. Intervals for the design variables

	Ra (μm)	Rq (μm)	Rt (μm)	Skewness	Kurtosis
Surface A	0.72	1.09	6.99	0.8	5.98
Surface B	1.94	2.35	12.77	0.17	3.59
Surface C	28.83	33.93	125.83	0.29	2.82

Table 2. Error in the pressure-drop repeatability test

Flow speed (m/s)	1.62	2.87	4.01	5.17	6.29	7.45	8.3
Error (%)	0.92	1.01%	0.08%	0.44%	0.10%	0.01%	0.16%

the Reynolds number (Re_m) varying from 24,000 to 113,000. The skin friction coefficient (C_f) of the tested panels were plotted against the Reynold's number in Figure 9. The hierarchy amongst the tested surfaces as a function of surface roughness is clearly apparent, as expected considering the roughness characteristics of these test surfaces.

4.1. Deviation

Precision uncertainty estimates for the pressure-drop measurements were made using the repeatability test. Seven replicate measurements were taken on the acrylic and SPC-coated panels. Error in pressure-drop repeatability was estimated based on the measured data using Equation 6. A very small error (maximum 1.01%) was found and included in Table 2.

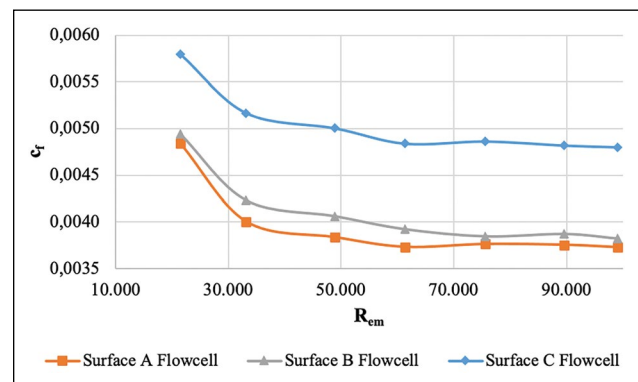
$$\text{Error} = \frac{\text{Test1} - \text{Test2}}{\text{Test1}} \times 100$$

5. CONCLUSIONS

An extensive experimental program was carried out to evaluate the pressure-drop methodology using UNEW's enhanced flow cell that had recently been modified to accommodate a new pressure-drop section and the Emerson Cavitation Tunnel's boundary layer measurement set-up using LDV. The methodology can be used to calculate the hydrodynamic performance (i.e., skin friction characteristics) of any type of flat surface with varying roughness profiles. The skin friction data can be provided for these surfaces in a short time, which can substitute the skin friction analysis based on the traditional boundary layer measurement method.

In order to evaluate the new methodology, three flat test panels with different surface finishes were analyzed. The results indicate the following conclusions:

- Calibration tests with the flow cell showed that the enhanced facility with the new stainless-steel test section can generate fully turbulent flow at the

**Figure 9.** The comparative friction coefficient of test panels as a function of flow speed.

pressure-drop measurement area. The calibration curves for the enhanced flow cell are represented by two reference velocities at the pressure-drop measurement section: the maximum inflow velocity measured at the center of the pressure drop section and the averaged velocity (or bulk velocity) determined from the spatially measured inflow velocities in the same section.

- The pressure-drop methodology clearly displayed a direct relationship between the tested surfaces' roughness and drag characteristics, with rougher surfaces having higher measured friction velocities.
- The relative merits of the measured surfaces (i.e., hierarchy of C_f for Surfaces A, B, and C) based on the ECT and flow cell are almost the same. This is extremely encouraging for the new measurement methodology (i.e., flow cell/pressure drop) as this will enable the relative merits of the surfaces to be evaluated with different coatings and biofilms effectively in a very short measurement time.

Future plans involve correlating the roughness characteristics of surfaces with drag performances. The correlation will be able to use the roughness functions for extrapolating results to full scale.

DATA AVAILABILITY STATEMENT

The published publication includes all graphics and data collected or developed during the study.

CONFLICT OF INTEREST

The author declared no potential conflicts of interest with respect to the research, authorship, and/or publication of this article.

ETHICS

There are no ethical issues with the publication of this manuscript.

FINANCIAL DISCLOSURE

The research leading to these results has received funding from the European Union's Seventh Framework Programme (FP7-OCEAN-2013), Project Seafront under Grand Agreement No: 614034.

REFERENCES

- Banerjee, I., Pangule, R. C., & Kane, R. S. (2011). Antifouling coatings: Recent developments in the design of surfaces that prevent fouling by proteins, bacteria, and marine organisms. *Advanced Materials*, 23(6), 690–718. [\[CrossRef\]](#)
- Candries, M. (2001). Drag, boundary layer and roughness characteristics of marine surfaces coated with antifoulings [Unpublished Doctoral Dissertation]. Newcastle University.
- Dean, R. B. (1978). Reynolds number dependence of skin friction and other bulk flow variables in two-dimensional rectangular duct flow. *Journal of Fluids Engineering*, 100(2), 215–223. [\[CrossRef\]](#)
- Harvald, S. A. (1983). Resistance and propulsion of ships. John Wiley & Sons.
- Monty, J. P. (2005). Developments in smooth wall turbulent duct flows [Unpublished Doctoral Dissertation]. University of Melbourne, Department of Mechanical and Manufacturing Engineering.
- Nikuradse, J. (1933). Laws of flow in rough pipes. VDI Forschungsheft.
- Politis, G., Atlar, M., Kidd, B., & Stenson, P. (2013, September 7-8). A multipurpose flume for the evaluation of hull coatings. 3rd International Conference on Advanced Model Measurement Technology for the Maritime Industry (AMT'13), Gdansk, Poland.
- Schultz, M. P., Bendick, J. A., Holm, E. R., & Hertel, W. M. (2011). Economic impact of biofouling on a naval surface ship. *Biofouling*, 27(1), 87–98. [\[CrossRef\]](#)
- Townsin, R. L. (2003). The ship hull fouling penalty. *Biofouling*, 19(1), 9–15. [\[CrossRef\]](#)
- Woods Hole Oceanographic Institution. (1952). Marine fouling and its prevention: Prepared for Bureau of Ships. George Banta Publishing Company.
- Zanoun, E., Nagib, S. H., & Durst, F. (2009). Refined cf relation for turbulent channels and consequences for high-Re experiments. *Fluid Dynamics Research*, 41(2), Article 021405. [\[CrossRef\]](#)